Journal of Organometallic Chemistry 694 (2009) 14–20

Contents lists available at ScienceDirect

Journal of Organometallic Chemistry

journal homepage: www.elsevier.com/locate/jorganchem

The synthesis, crystal structures and NMR spectroscopic investigation of 3,7,10-trimethylsilatranes and carbasilatranes

Ilona Kovács [a,*], Eberhard Matern [b], Ewald Sattler [b], Christopher E. Anson [b], László Párkányi [c]

[a] Budapest University of Technology and Economics, Department of Inorganic and Analytical Chemistry, H-1111, Szt. Gellér tér 4, Budapest, Hungary
[b] Universität Karlsruhe (TH), Institut für Anorganische Chemie, D-76128, Engesserstr. 15, Karlsruhe, Germany
[c] Institute of Chemistry, Chemical Research Center, Hungarian Academy of Sciences, H-1025, Pusztaszeri út 59-67, Budapest, Hungary

ARTICLE INFO

Article history:
Received 4 July 2008
Accepted 29 September 2008
Available online 4 October 2008

Keywords:
Trimethylsilatranes
Carbasilatranes
NMR spectroscopy
X-ray scattering

ABSTRACT

The first representatives of aryloxy-trimethylsilatranes, $C_6H_5OSi[OCH(CH_3)CH_2]_3N$, of aryloxy-carbasilatranes, $C_6H_5OSi(CH_2CH_2CH_2)(OCH_2CH_2)_2N$, and a number of novel 3,7,10-trimethylsilatranes ($RSi[OCH(CH_3)CH_2]_3N$) and carbasilatranes ($RSi(CH_2CH_2CH_2)(OCH_2CH_2)_2N$) have been prepared and characterised, both structurally and by NMR spectroscopy. The influence of various Si substituents (R = alkyl, aryl, alkoxy and aryloxy) as well as the influence of the substitution in the skeleton of the trimethylsilatranes and carbasilatranes on the chemical shift in the ^{29}Si, ^{1}H and ^{13}C NMR spectra has been investigated. The crystal structures of both diastereomers of phenyl-3,7,10-trimethylsilatrane and of the symmetrical isomer of *p*-tolyl-3,7,10-trimethylsilatrane were determined by X-ray diffraction after separation of the diastereomers by means of HPLC. All three crystal structures are centrosymmetric.

1. Introduction

The silatranes $RSi(OCH_2CH_2)_3N$ adopt a special position among the hypervalent neutral penta- and hexa-coordinated silicon compounds as a result of the characteristic structure of their bonding [1]. The central silicon atom is linked by means of three triatomic bridges to a nitrogen atom, the free electron pair of which is engaged in a relatively weak, easily distortable, coordinative bond to the silicon atom, dependent on the conditions of aggregation [2]. The length and strength of this bond also depends on the axial substituent R on the silicon atom and upon the properties of the bridges, *i.e.* on the electronic influence of the neighbouring O, N, C atoms in the α-positions defining the equatorial plane, on the number of atoms present in the bridges, and possibly also on steric influences [3]. This Si←N interaction seems to be responsible for many important chemical [4] and biological [5] properties of the silatranes. Some aspects of this dative bond between Si and N are still not fully understood, therefore the synthesis of new silatranes as well as the comprehensive characterisation of as many as possible derivatives is highly desirable. Recently, silatranes have found some applications in material science [6].

In the present paper, the preparation and characterisation of several 3,7,10-trimethylsilatranes and carbasilatranes are reported, and the influences of various substituents (R = alkyl, aryl, alkoxy, aryloxy) and the substitution in the skeleton of the trimethylsilatranes and carbasilatranes on the chemical shift in the ^{29}Si, ^{1}H and ^{13}C NMR spectra are discussed. Additionally, the single crystal structure investigations of the diastereomers of the phenyl- and *p*-tolyl-3,7,10-trimethylsilatranes are reported. It is of special value that we can present data for several compounds as well in the solid as in the liquid state, and such can consider their properties from a more general point of view.

2. Results and discussion

2.1. Synthesis of investigated compounds

The compounds investigated in this study are presented on Fig. 1. The alkyl-trimethylsilatranes **1a**–**5a** and the aryl-trimethylsilatranes **6a**, **7a** were prepared from silicon-substituted trimethoxysilanes and tri*iso*propanolamine by a modification of the method of Frey [7], the alkoxy-trimethylsilatranes **8a**, **9a** were synthesised from tetraethoxysilane, tri*iso*propanolamine and the appropriate alcohol using a modification of the method of Voronkov and Zelchan [8]. The carbasilatranes **1b** and **6b**–**8b** were obtained from silicon-substituted (γ-chloropropyl)dimethoxysilanes and diethanolamine (in the presence of triethylamine as HCl acceptor) using improved literature methods [9]. To our knowledge no aryloxy-trimethylsilatranes and aryloxy-carbasilatranes have been previously described. We report here the syntheses of the first representatives of these compounds. The synthesis of phenoxy-trimethylsilatrane **10a** was not possible using the same route as for the alkoxy-trimethylsilatranes, but the compound could be prepared Eq. (1):

* Corresponding author. Tel.: +36 1 463 1294; fax: +36 1 463 3642.
E-mail address: ikovacs@mail.bme.hu (I. Kovács).

0022-328X/$ - see front matter © 2008 Elsevier B.V. All rights reserved.
doi:10.1016/j.jorganchem.2008.09.055

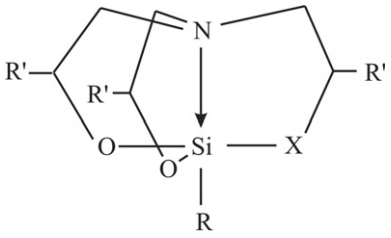

R	R'= CH_3 X = O	R'= H X = CH_2
CH_3	**1a** [4a]	**1b** [4a]
$Cl(CH_2)_3$	**2a**	
$HS(CH_2)_3$	**3a**	
$CH_2{=}C(CH_3)COO(CH_2)_3$	**4a**	
$H_2N(CH_2)_2NH(CH_2)_3$	**5a**	
C_6H_5	**6a** [4a]	**6b** [4a]
p-$CH_3C_6H_4$	**7a** [11]	**7b** [12]
CH_3O	**8a** [10]	**8b** [4a]
n-$C_8H_{17}O$	**9a**	
C_6H_5O	**10a**	**10b**

Fig. 1. The investigated 3,7,10-trimethylsilatranes and carbasilatranes.(See above-mentioned references for further information[10]).

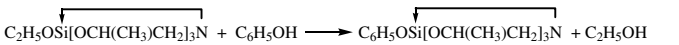

(1)

The phenoxy-carbasilatrane **10b** was synthesised in the following manner:

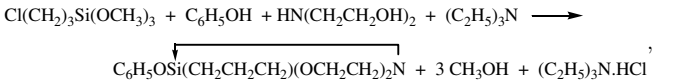

(2)

The new compounds were characterised by ^{1}H, ^{13}C, ^{29}Si NMR, IR, MS and elemental analyses. The syntheses of the 3,7,10-trimethylsilatranes lead to mixtures of diastereomers (Fig. 2).

The symmetrical diastereomer has idealised C_3 molecular symmetry, the asymmetric only C_1. The theoretical isomeric ratio is ***sym*:*asym*** = 1:3. The diastereomers of compounds **6a** and **7a** could be separated by means of HPLC chromatography; the minor diastereoisomers had the shorter retention time. Single crystals suitable for X-ray analysis could be obtained from both stereoisomers of **6a** and from the minor stereoisomer of **7a**.

Table 1
Crystal data and structure refinement of $\mathbf{6a_{sym}}$, $\mathbf{6a_{asym}}$ and $\mathbf{7a_{sym}}$.

Data	$\mathbf{6a_{sym}}$	$\mathbf{6a_{asym}}$	$\mathbf{7a_{sym}}$
Empirical formula	$C_{15}H_{23}NO_3Si$	$C_{15}H_{23}NO_3Si$	$C_{16}H_{25}NO_3Si$
Formula weight	293.43	293.43	307.46
Temperature, K	100(2)	100(2)	293(2)
Radiation, wavelength, Å	Mo Kα, λ = 0.71073	Mo Kα, λ = 0.71073	Cu Kα, λ = 1.5418
Crystal system	Monoclinic	Monoclinic	Monoclinic
Space group	$P2_1/c$	$P2_1/n$	$P2_1/c$
a(Å)	10.9566(5)	18.3613(19)	11.824(1)
b(Å)	16.9950(8)	9.7768(10)	12.161(1)
c(Å)	16.6884(8)	18.6127(18)	13.116(1)
β(°)	97.491(1)	113.059(2)	116.55(1)
Volume, Å^3	3081.0(3)	3074.3(5)	1687.1(3)
Z	8	8	4
D_{calc}, Mg m^{-3}	1.265	1.268	1.210
μ, mm^{-1}	0.159	0.160	1.306
F(000)	1264	1264	664
Crystal colour	Colourless	Colourless	Colourless
Crystal description	Chunk	Needle	Prism
Crystal size, mm	0.47 × 0.44 × 0.39	0.22 × 0.08 × 0.06	0.50 × 0.40 × 0.15
$2\theta_{max}$ (°)	56.02	54.04	151.50
Reflections collected	15327	11347	3693
R_{int}	0.0254	0.0861	0.0287
Unique reflections	6935	6144	3417
Reflections $I > 2\sigma(I)$	5760	2166	3100
Final wR_2 (all data)	0.1418	0.0857	0.1524
S (all data)	1.024	0.875	1.041
Final R_1 [$I > 2\sigma(I)$]	0.0521	0.0591	0.0502
Largest difference in peak/hole, e Å^{-3}	0.49/−0.56	0.73/−0.42	0.39/−0.37

2.2. Crystal structure determinations

Crystallographic data for $\mathbf{6a_{sym}}$, $\mathbf{6a_{asym}}$ and $\mathbf{7a_{sym}}$ are summarised in Table 1, the molecular diagrams are depicted in Fig. 3 and selected bond distances and angles are listed in Table 2. In the crystal structures of both $\mathbf{6a_{sym}}$ and $\mathbf{6a_{asym}}$ there are two independent molecules in the asymmetric unit.

Silatranes with an unsubstituted atrane skeleton usually form ordered structures. When they are disordered, the carbon atoms α to the nitrogen appear in split positions. These partially filled atom sites are positioned on both sides of the planes formed by Si, O, C (β to N) and N. Methyl substitution at the C3, C7, C10 atoms dramatically changes this situation as the disorder mostly affects these methyl substituted carbons (and the methyl moiety) and these now appear on both sides of the Si, O, C (α to N) and N chains.

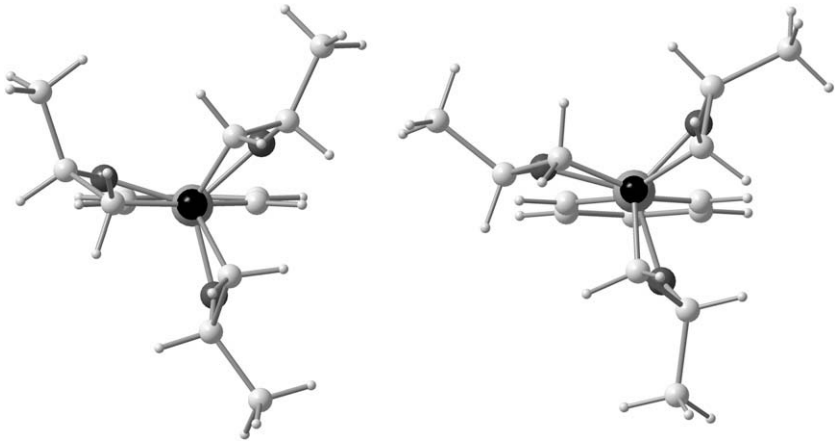

Fig. 2. Symmetrical (right) and asymmetrical (left) diastereomers of silatranes.

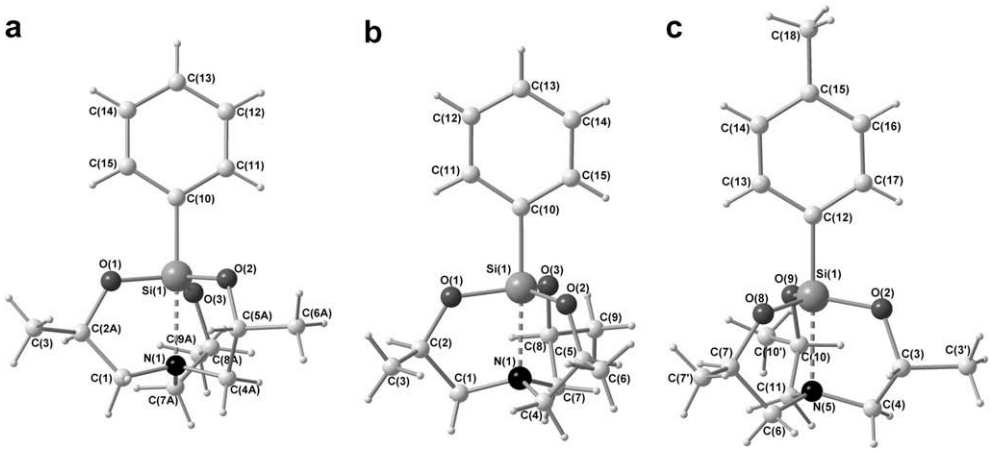

Fig. 3. Molecular structures of **6a$_{sym}$** (a), **6a$_{asym}$** (b) and **7a$_{sym}$** (c). In (a) and (b), Molecule 1 from the asymmetric unit is shown; in (a) and (c) atoms of the minor disorder components are omitted for clarity.

Table 2
Selected bond lengths (Å) and angles (°).

Compound	**6a$_{sym}$/1**	**6a$_{sym}$/2**	**6a$_{asym}$/1**	**6a$_{asym}$/2**	**7a$_{sym}$**
Si1 ← N5	2.155(1)	2.164(1)	2.144(3)	2.182(3)	2.223(2)
Si1–O2	1.662(1)	1.663(1)	1.657(3)	1.656(3)	1.648(2)
Si1–O8	1.657(1)	1.656(1)	1.664(3)	1.659(3)	1.655(1)
Si1–O9	1.665(1)	1.663(1)	1.673(3)	1.659(3)	1.655(1)
Si1–C12	1.902(2)	1.893(2)	1.895(4)	1.889(4)	1.887(2)
O8–Si1–O2	118.06(7)	117.82(6)	118.8(1)	118.2(2)	119.36(9)
O2–Si1–O9	120.29(7)	118.07(8)	117.6(2)	118.7(1)	117.90(9)
O8–Si1–O9	117.64(7)	119.76(8)	119.7(2)	118.7(2)	116.96(9)
O2–Si1–C12	96.67(6)	97.52(7)	98.1(2)	97.4(2)	98.25(8)
O8–Si1–C12	98.36(6)	97.46(7)	96.0(2)	96.1(2)	97.73(7)
O9–Si1–C12	95.07(6)	95.94(6)	95.8(2)	97.5(2)	98.19(7)
O2–Si1 ← N5	83.43(6)	82.78(6)	83.8(1)	83.1(1)	82.04(7)
O8–Si1 ← N5	83.66(5)	83.57(6)	82.8(2)	82.9(1)	81.75(7)
O9–Si1 ← N5	82.85(6)	82.74(6)	83.6(1)	83.0(1)	82.05(6)
C12–Si1 ← N5	177.62(6)	178.62(6)	178.1(2)	179.0(2)	179.48(7)

Both molecules in the asymmetric unit of **6a$_{sym}$** are disordered, the site occupation factors (s.o.f.) are 0.74:0.26 for Molecule 1 and 0.63:0.37 for Molecule 2. One molecule in the asymmetric unit of **6a$_{asym}$** is ordered, while the second is disordered with a s.o.f. ratio of 0.70:0.30. There is only one molecule in the asymmetric unit of **7a$_{sym}$**. The atrane skeleton is disordered and the disordered atoms have a s.o.f. ratio of 0.665:0.335.

All three crystal structures are centrosymmetric, and half the sites in the unit cell should contain one enantiomer, with the other sites containing the opposite enantiomer. The observed disorder corresponds to a small proportion of the "wrong" enantiomer in a given site. In all three cases, the two enantiomers have a very similar external shape, with the methyl substituents in similar positions on the periphery of the molecule, so that such packing errors do not greatly affect the neighbouring molecules, and such disorder is therefore not unlikely.

The Si ← N transannular bonds vary over the range 2.14–2.22 Å. In particular, these bond lengths differ significantly between the two independent molecules in the structures of both compounds **6a$_{sym}$** and **6a$_{asym}$**. The silatrane skeleton undergoes rapid conformational changes (flapping of the O–C–C–N chains) in solution, and it appears that on crystallization the demands of the crystal packing results in particular "snapshots" of this motion being frozen out. This may account for the different molecular geometries. A room temperature crystal structure of **6a$_{sym}$** [12] showed no apparent disorder, though the accuracy of the data was limited and some of the atomic displacement parameters were rather high, suggesting that disorder was present but unresolved. The Si ← N bonds at 2.167(3) and 2.182(3) Å are longer than the values in the present low temperature study, 2.155(1) and 2.164(1) Å, respectively.

The crystal structure of the major stereoisomeric component of **7a$_{asym}$** was published earlier [11]. The Si ← N distance, 2.236(3) Å, is longer by 0.013 Å than in **7a$_{sym}$**, possibly due to a more strained atrane skeleton, but crystal packing effects may be the primary cause (see below).

In comparison with the unsubstituted silatranes the methyl substitution on the C atoms 3, 7 and 10 of the skeleton in the *p*-tolyl derivatives causes a considerable lengthening of the Si–N distance (**7c**: 2.169 Å [11]). This effect cannot be observed for the phenyl derivatives (**6c** α: 2.193 Å [13a], **6c** β: 2.156 Å [13b], **6c** γ: 2.132 Å [13c]). More comprehensive comparison is not possible because not sufficient structural data are known.

It has been established earlier [14] that the displacement of the silicon atom out of the plane of its three equatorial oxygens (ΔSi) and the deviation of the nitrogen from the plane of its carbon substituents (ΔN) are dependent on the length of the Si ← N dative bond. Short dative bonds were found to result in more coplanar SiO_3 moieties while, conversely, the nitrogen becomes less tetrahedral for longer Si ← N bonds. Here, this rule holds approximately for ΔSi, but no such trend can be observed for ΔN (Fig. 4).

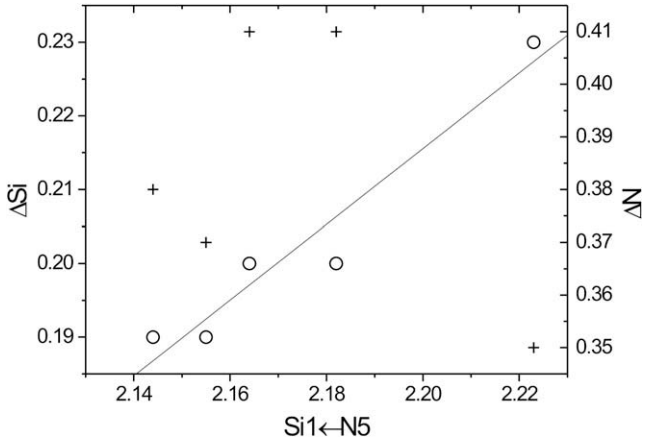

Fig. 4. The distance of Si from the plane of the oxygen atoms (ΔSi, Å; circles, line of best fit) and the distance of *N* from the plane of C4, C6 and C11 (ΔN, Å; +) as a function of the Si ← N approach (Å) in **6a$_{sym}$**, **6a$_{asym}$** and **7a$_{sym}$** (see Table 2).

2.3. NMR spectroscopic studies

2.3.1. ^{29}Si NMR spectra

Structural data [1a] show that electronegative substituents on Si cause a shortening of the Si–N distance in silatranes. However, variations in the bridges of the silatrane skeleton cause stronger changes in the geometry of the heterocycle and in the Si–N distance than those of the electronic or steric properties of the substituent in axial position of the silatrane skeleton. As chemical shifts react sensitively to changes in the geometry in the neighbourhood of the nucleus being measured, changes of the Si–N distances should be reflected in changes of the value of δ^{29}Si. Additionally, all silatranes should show a strong high field shift of δ^{29}Si due to their nearly trigonal bipyramidal pentacoordinated Si atoms as compared to the correspondingly substituted triethoxysilanes [15].

The values of the ^{29}Si chemical shifts of the 3,7,10-trimethylsilatranes, carbasilatranes and some sil-atranes with unsubstituted skeletons are compared in Table 3. The signals of the compounds **2a**–**10a** are shifted to high field compared to the methyl derivative **1a**. This corresponds to the expected high-field shift of the ^{29}Si resonances with increasing electronegativity of the substituents. If the substituent is linked *via* an oxygen atom to Si, as in **8a**–**10a**, a strong high field shift results, and the strongest effect is observed for R = C_6H_5O. Comparing the 3,7,10-trimethylsilatranes with unsubstituted silatranes shows that there is no uniform trend. The dependence of the chemical shift values from the polarity of the solvent has not been systematically investigated. In any case, it is small and did not show an uniform trend when changing from $CDCl_3$ to C_6D_6.

The ^{29}Si chemical shifts for the carbasilatranes **1b**, **6b**–**8b** and **10b** show a dependency comparable to that in the series of the trimethylsilatranes. The exchange of an equatorial oxygen against a methylene group results in the expected strong low field shift.

The very low variation in the ^{29}Si chemical shifts strongly suggests that in solution the silatranes considered here all have rather similar Si–N distances. It must therefore be the crystal packing which is of primary importance in determining the conformation of the three organic bridges between the Si and N atoms, and thus the Si–N distance; therefore, this distance is not intrinsically imposed by the substitution pattern. The Si–N interaction can thus be considered highly plastic, with the bond length varying readily in response to different crystal packing environments. This is particularly apparent when comparing the significantly different Si–N distances for the crystallographically-independent molecules in the structures of either **6a$_{sym}$** or **6a$_{asym}$**; in these cases the molecules are chemically identical, and the differences in Si–N can only result from packing effects.

2.3.2. ^{1}H NMR spectra

The ^{1}H NMR spectroscopical investigations of a series of silatranes of the type RSi(OCH$_2$CH$_2$)$_3$N have shown that the signals of the NCH$_2$ and OCH$_2$ protons of the silatrane cage each fall in a small range of 0.25 ppm, and that with increasing electronegativity of the substituents a low field shift can be observed [16]. As demonstrated by thorough structural investigations of silatranes [1a], the increasing electronegativity of the axial substituent R leads to a shortening of the Si–N bond and thus to an increasing transannular donor–acceptor interaction between the N and the Si atom.

The introduction of methyl groups in the positions 3, 7 and 10 of the silatrane cage causes the loss of the C_3 symmetry in case of the asymmetrical diastereomer, resulting in more complex ^{1}H NMR spectra. The ^{1}H NMR spectra of the trimethylsilatranes **1a**–**10a** all show the same pattern, and R substituents on Si in the axial position of the silatrane framework have just a minor influence. In all spectra, the signals from the protons of the silatrane cage are well separated, which allows for a reliable integration with respect to the group intensities. In all cases, mixtures of the symmetrical and the asymmetrical diastereomers are present (Fig. 2). For the symmetrical structure, only one spectrum would be expected for all three bridges, whereas each bridge of the asymmetrical isomer will give rise to a distinct spectrum. Indeed, four partial spectra are observed which overlap only to some extent. These all have nearly the same intensity, which gives a ratio of 1:3 for the symmetrical to the asymmetrical isomer. By means of ^{1}H COSY spectra, and using the ^{1}H spectral data from the separated isomers of **6a** and **7a**, signals could be assigned both to the respective diastereomers and also to the different protons within the silatrane bridges. By means of an iterative optimization [17] the chemical shifts and the coupling constants for **6a** in Table 4 were obtained.

The ^{1}H NMR spectrum of a carbasilatrane consists of two independent parts, one resulting from the –(CH$_2$)$_3$– bridge and the other from the two –O(CH$_2$)$_2$– bridges of the cage, which are of AA′MM′XX′ and ABXY types, respectively. The apparent C_S mirror symmetry (with the atoms Si–C–C–C–N in the mirror plane) is not caused by a rigid molecular skeleton but by the high flexibility of the three bridges in solution at room temperature; only the effective symmetry for the "average" of the fast interchanging conformations is observed. This is mostly due to the fact that non-substituted five-membered envelope rings have an even lower energy threshold for inversion than the analogous six-membered rings, that no sterically-demanding substituents are enforcing certain conformations, that no rigid building blocks such as carbonyl groups are present, and that the substituent on the Si atom can rapidly rotate about the Si–C bond and therefore does not cause a lowering of the symmetry. Due to their different chemical environments, with the –(CH$_2$)$_3$– bridge on one side and the second –O(CH$_2$)$_2$– bridge on the other, each of the geminal H atoms of the –O(CH$_2$)$_2$– bridge has a different average value for its chemical shift in spite of the

Table 3
^{29}Si NMR chemical shifts [ppm] of the silatranes (**1**–**10**) **a**, **b**, **c** (solvent $CDCl_3$).

	R	a		b	c
		sym.	*asym.*		
1	CH_3	−66.3	−64.3	−29.1 [4a]	−65.7 [4a]
2	$Cl(CH_2)_3$	−71.6	−69.1		−68.2 [4a]
3	$HS(CH_2)_3$	−70.0	−67.5		−66.7
4	$CH_2{=}C(CH_3)COO(CH_2)_3$	−70.2	−67.7		
5	$H_2NCH_2CH_2NH(CH_2)_3$	−68.6	−66.2		
6	C_6H_5	−83.8	−81.4 [4a]	−45.6 [4a]	−80.5 [4a]
7	*p*-$CH_3C_6H_4$	−83.1	−80.6 [11]	−45.0 [12]	−80.6 [11]
8	CH_3O	−96.7	−94.9	−63.1	−95.4 [4a]
9	*n*-$C_8H_{17}O$	−97.0	−95.1		
10	C_6H_5O	−98.4	−96.7	−67.6	−99.3 [4a]

[a] RSi[OCH(CH$_3$)CH$_2$]$_3$N; **b** RSi(CH$_2$CH$_2$CH$_2$)(OCH$_2$CH$_2$)$_2$N; **c** RSi(OCH$_2$CH$_2$)$_3$N.

Table 4
^{1}H NMR data of $C_6H_5Si[OCH^3(CH_3{}^4)CH_2{}^{1,2}]_3N$ **6a** (solvent $CDCl_3$).

	sym.	asym.		
δ_1	2.842	3.001	3.069	2.901
δ_2	2.313	2.727	2.405	2.385
δ_3	4.012	4.254	4.231[a]	4.072
δ_4	1.235	1.317	1.221[b]	1.259[b]
$J_{1,2}$ (Hz)	−12.21	−13.26	−12.28	−12.37
$J_{1,3}$ (Hz)	3.91	6.56	4.06	4.05
$J_{2,3}$ (Hz)	11.05	5.41	11.03	11.15
$J_{3,4}$ (Hz)	6.05	6.56	6.04	6.10
$C_6H_5\delta$	7.246[c] and 7.781[c]			

[a] Not iterated.
[b] Assignment uncertain, values may be exchanged.
[c] Maximum peak in the complex multiplet, no assignment sym/asym possible.

Table 5
^{1}H NMR data of $C_6H_5Si(CH_2^{1,2}CH_2^{3,4}CH_2^{5,6})(OCH_2^{7,8}CH_2^{9,10})_2N$ **6b** (solvent C_6D_6).

	(ppm)		(Hz)
δ_1	0.804	$J_{1,2}$	−16.08
δ_2	0.804	$J_{1,3}$	7.698
δ_3	1.699	$J_{1,4}$	6.338
δ_4	1.699	$J_{3,4}$	−12.522
δ_5	2.613	$J_{3,5}$	7.259
δ_6	2.613	$J_{3,6}$	5.021
δ_7	3.781	$J_{5,6}$	−10.766
δ_8	3.869	$J_{7,8}$	−11.19
δ_9	2.778	$J_{7,9}$	6.532
δ_{10}	2.843	$J_{7,10}$	5.031
		$J_{9,10}$	−12.572
		$J_{8,9}$	5.070
		$J_{8,10}$	6.335

molecular dynamic. A higher symmetry than that for the ABXY type is not possible for this part of the spectrum. The fitting for **6b** yields identical results for the –$(CH_2)_3$– bridge (Table 5), whether or not C_S symmetry was imposed [17]. Even if such parameters were refined in the calculations, the calculated values for the $^4J_{HH}$ coupling constants never differed significantly from zero.

The exchange of an electronegative oxygen atom for a CH_2 group leads as expected to a high-field shift for both the neighbouring methylene protons and those of the NCH_2 group. The chemical shift of the NCH_2 protons is close to that of simple silatranes and thus confirms that a transannular Si ← N interaction is also present in the novel carbasilatranes presented here.

2.3.3. ^{13}C NMR spectra

As was the case for the ^{1}H NMR spectra, in the ^{13}C NMR spectra of the 3,7,10-trimethylsilatranes only one spectrum is again expected for all three bridges of the symmetrical isomer, whereas each bridge of the asymmetrical isomer must have its own spectrum. Due to the more electronegative oxygen, the signals of the OCH_2 group appear at lower field than those of the NCH_2 group. For compounds **6a** and **7a**, the ^{13}C spectra of the separated isomers again support the assignment. For the compounds **2a**–**5a** and **8a**–**10a** the assignment was derived from ^{1}H/^{13}C correlation and ^{13}C DEPT spectra. A more advanced assignment of the signals to the particular bridges is not possible.

Compared to those silatranes with no substituents on the ring atoms, the values of the ^{13}C NMR signals of the OCH_2 and NCH_2 groups in the carbasilatranes show only a weak low field shift; the signals for the $SiCH_2$ or CCH_2C groups, respectively, appear at considerably higher field.

3. Conclusion

The present study involves the preparation of several novel 3,7,10-trimethylsilatranes (**2a**–**5a**, **9a**) and of the carbasilatrane **10b**. The synthesis of phenoxy-trimethylsilatrane **10a** was not possible using the same route as for alkoxy-trimethylsilatranes. However, the compound could be isolated from the reaction between ethoxy-trimethylsilatrane and phenol. Thorough ^{29}Si, ^{1}H and ^{13}C NMR investigations show the influence of various substituents R and of the substitution in the skeleton of trimethylsilatranes and carbasilatranes on the chemical shift of the measured nuclei. The introduction of methyl groups in positions 3, 7 and 10 of the silatrane cage leads to mixtures of diastereomers causing complex ^{1}H NMR spectra. By means of ^{1}H COSY spectra and of ^{1}H spectra of the separated isomers for **6a** and **7a** the signal groups could be assigned to both diastereomers and also to the different protons attached to the silatrane bridges. The crystal structures of both diastereomers of phenyl-3,7,10-trimethylsilatrane **6a** and of the symmetrical isomer of *p*-tolyl-3,7,10-trimethylsilatrane $\mathbf{7a_{sym}}$ were determined by X-ray diffraction. (The crystal structure of the asymmetrical isomer of $\mathbf{7a_{asym}}$ was published earlier [11].) All three crystal structures are centrosymmetric. The Si ← N transannular bonds vary over the range from 2.14 to 2.22 Å.

4. Experimental

4.1. General

^{1}H, ^{13}C and ^{29}Si NMR spectra were recorded on Bruker AC 250 and AMX 300 spectrometers (standard: external TMS), IR spectra were measured as KBr pellets with a PYE UNICAM SP 2000 spectrometer and mass spectra were obtained with a JEOL JMS 01SG-2 instrument. HPLC separations were performed using a Hitachi chromatograph equipped with a normal phase Silica gel column and an UV detector (254 nm); eluant dichloromethane: hexane:THF = 100:20:4.

Crystallographic data for $\mathbf{6a_{sym}}$, $\mathbf{6a_{asym}}$ were collected on a Bruker SMART Apex CCD diffractometer, and for $\mathbf{7a_{sym}}$ on an Enraf–Nonius CAD4 diffractometer. Crystal data, data collection and refinement parameters are summarised in Table 1. The structures were solved by direct methods [18a] and were refined by full-matrix least-squares on F^2 using SHELXTL [18b].

Ethoxy-trimethylsilatrane was prepared according to literature procedures [8].

4.2. Synthesis of compounds *2a*–*5a*, *8a*–*10a*, and *10b*

*4.2.1. $X(CH_2)_3OSi[OCH(CH_3)CH_2]_3N$ (**2a**–**5a**)*

0.02 mol of the corresponding $X(CH_2)_3Si(OMe)_3$ was reacted with 0.02 mol tri*iso*propanolamine in xylene (20 mL) at 110 °C with a catalytic amount of KOH. The methanol formed was removed using a Marcusson device, and the reaction mixture was then stirred for 1–2 h at 110 °C. The solvent was removed *in vacuo* and the remaining oil worked up by distillation.

2a (X: Cl) Yield: 4.57 g (78%), b.p. 115–116 °C/0.02 mbar. Anal. Calc. for $C_{12}H_{24}ClNO_3Si$: C, 49.05; H, 8.23; N, 4.77; Si, 9.56. Found: C, 49.12; H, 8.50; N, 4.97; Si, 9.59%. $^{13}C\{^1H\}$ NMR ($CDCl_3$): δ 63.9 (*O*CH *sym*), 67.3, 65.5, 65.4 (*O*CH *asym*), 59.5 (NCH_2 *sym*), 65.7, 62.3, 62.3 (NCH_2 *asym*), 20.9 (CH_3 *sym*), 23.8, 21.3, 21.0 (CH_3 *asym*), 48.8 ($ClCH_2$), 29.6 (CCH_2C), 14.6 ($SiCH_2$). IR (cm^{-1}): 1464 m, 1380 s, 1160 s, 1115 s, 1098 m, 885 s, 780s, 662 m, 428 w. EI-MS: *m*/*z* (relative abundance, %) 293.2 (5), 295.2 (2) [M^+], 216.1 (100) [M^+-$Cl(CH_2)_3$].

3a (X: SH) Yield: 4.65 g (80%), b.p. 121–122 °C/0.02 mbar. Anal. Calc. for $C_{12}H_{25}NO_3SSi$: C, 49.45; H, 8.64; N, 4.81; Si, 9.64. Found: C, 49.98; H, 8.93; N, 5.09; Si, 9.40%. $^{13}C\{^1H\}$ NMR ($CDCl_3$): δ 63.2 (*O*CH *sym*), 66.6, 64.9, 64.7 (*O*CH *asym*), 58.7 (NCH_2 *sym*), 65.0, 61.5, 61.5 (NCH_2 *asym*), 20.3 (CH_3 *sym*), 23.1, 20.7, 20.4 (CH_3 *asym*), 30.6 (SCH_2), 28.3 (CCH_2C), 16.1 ($SiCH_2$). IR (cm^{-1}): 1460 m, 1381 m, 1160 s, 1115 s, 1098 m, 885 s, 780s, 660 m, 428 w. EI-MS: *m*/*z* (relative abundance, %) 291.2 (2) [M^+], 216.2 (100) [M^+-$HS(CH_2)_3$].

4a (X: CH_2=C(CH_3)COO) Yield: 4.87 g (71%), b.p. 128–129 °C/0.02 mbar. Anal. Calc. for $C_{16}H_{29}NO_5Si$: C, 55.95; H, 8.51; N, 4.08; Si, 8.18. Found: C, 55.33; H, 8.85; N, 4.79; Si, 8.02%. $^{13}C\{^1H\}$ NMR ($CDCl_3$): δ 63.2 (OCH_2 *sym*), 66.6, 64.9, 64.8 (OCH_2 *asym*), 58.6 (NCH_2 *sym*), 65.2, 61.5, 61.4 (NCH_2 *asym*), 20.2 (CH_3 *sym*), 23.1, 20.5, 20.3 (CH_3 *asym*), 167.5 (*C*OO), 136.7 (CH_2=*C*), 124.6 (CH_2=C), 67.9 ($COCH_2$), 24.3 (CCH_2C), 18.3 (=CCH_3), 12.5 ($SiCH_2$). IR (cm^{-1}): 1460 m, 1380 m, 1158 s, 1116 s, 1100 m, 883 s, 775s, 660 m, 423 w. EI-MS: *m*/*z* (relative abundance, %) 343.3 (3) [M^+], 216.2 (100) [M^+-CH_2=C(CH_3)COO$(CH_2)_3$].

5a (X: $H_2N(CH_2)_2NH$) Yield: 5.33 g (84%), b.p. 145–146 °C/0.01 mbar. Anal. Calc. for $C_{14}H_{31}N_3O_3Si$: C, 52.96; H, 9.84; N,

13.23; Si, 8.85. Found: C, 51.91; H, 9.55; N, 13.01; Si, 8.21%. $^{13}C\{^1H\}$ NMR ($CDCl_3$): δ 63.3 (O*C*H *sym*), 66.8, 65.0, 64.9 (O*C*H *asym*), 58.9 (N*C*H_2 *sym*), 65.2, 61.8, 61.6 (N*C*H_2 *asym*), 20.3 (*C*H_3 *sym*), 23.1, 20.7, 20.4 (*C*H_3 *asym*), 53.0, 52.6, 42.1(RN*C*H_2), 25.3 (C*C*H_2C), 13.6 (Si*C*H_2). IR (cm^{-1}): 1461 m, 1379 m, 1158 s, 1112 s, 1095 m, 886 s, 780 s, 662 w, 425 w. EI-MS: *m*/*z* (relative abundance, %) 216.2 (100) [M^+- $H_2N(CH_2)_2NH(CH_2)_3$], 287.3 (30) [M^+-NH_2CH_2].

4.2.2. $CH_3OSi[OCH(CH_3)CH_2]_3N$ (**8a**)

A solution of 1.52 g (0.01 mol) tetramethoxysilane and 1.91 g (0.01 mol) tri*iso*propanolamine in 10 mL xylene was heated to 100–110 °C. After addition of KOH, the methanol formed was distilled off. The residue was recrystallised from *n*-hexane. Yield: 1.78 g (72%), m.p. 92–94 °C. Anal. Calc. for $C_{10}H_{21}NO_4Si$: C, 48.56; H, 8.56; N, 5.66; Si, 11.35. Found: C, 49.22; H, 9.02; N, 5.78; Si, 10.83%. $^{13}C\{^1H\}$ NMR ($CDCl_3$): δ 63.9 (O*C*H_2 *sym*), 67.0, 65.4, 65.3 (O*C*H_2 *asym*), 59.6 (N*C*H_2 *sym*), 65.7, 62.4, 62.1 (N*C*H_2 *asym*), 20.9 (*C*H_3 *sym*), 23.9, 21.2, 21.0 (*C*H_3 *asym*), 51.5 (O*C*H_3). IR (cm^{-1}): 1464 m, 1378 m, 1162 s, 1115 s, 1098 s, 888 s, 791s, 660 w, 425 w. EI-MS: *m*/*z* (relative abundance, %) 247.1 (15) [M^+], 216.1 (100) [M^+-CH_3O].

4.2.3. $C_8H_{17}OSi[OCH(CH_3)CH_2]_3N$ (**9a**)

A solution of 2.08 g (0.01 mol) tetraethoxysilane, 1.91 g (0.01 mol) tri*iso*propanolamine and 1.43 g (0.011 mol) octylalcohol in xylene (10 mL) was heated to 100–110 °C. After addition of KOH, the ethanol formed was distilled off. The reaction mixture was worked up by distillation. Yield: 2.59 g (75%), b.p. 123–125 °C/0.02 mbar. Anal. Calc. for $C_{17}H_{35}NO_4Si$: C, 59.09; H, 10.21; N, 4.05; Si, 8.13. Found: C, 59.62; H, 10.67; N, 4.15; Si, 8.36%. $^{13}C\{^1H\}$ NMR ($CDCl_3$): δ 63.4 (O*C*H *sym*), 66.5, 65.0, 64.9 (O*C*H *asym*), 59.0 (N*C*H_2 *sym*), 65.1, 61.8, 61.6 (N*C*H_2 *asym*), 20.2 (*C*H_3 *sym*), 23.2, 20.6, 20.4 (*C*H_3 *asym*), 63.2 (*C*H_2OSi) 32.7, 31.8, 29.6, 29.3, 25.9, 22.6, (R*C*H_2), 14.1 (R*C*H_3). IR (cm^{-1}): 1460 m, 1376 m, 1150 s, 1115 s, 1100 m, 886 s, 784 s, 672 w. EI-MS: *m*/*z* (relative abundance, %) 345.2 (7) [M^+], 216.1 (100) [M^+-$C_8H_{17}O$].

4.2.4. $C_6H_5OSi[OCH(CH_3)CH_2]_3N$ (**10a**)

6.53 g (0.025 mol) ethoxy-trimethylsilatrane dissolved in 50 mL xylene was added to a solution of 2.35 g (0.025 mol) phenol in 50 mL xylene. The mixture was heated to 100 °C. After adding a catalytic amount of KOH, the ethanol formed was distilled off using a Marcusson device. The residue was recrystallised from *n*-hexane. Yield: 2.86 g (37%), m.p. 117–119 °C. Anal. Calc. for $C_{15}H_{23}NO_4Si$: C, 58.21; H, 7.49; N, 4.53; Si, 9.07. Found: C, 58.47; H, 7.21; N, 4.43; Si, 8.73%. $^{13}C\{^1H\}$ NMR ($CDCl_3$): δ 63.7 (O*C*H *sym*), 68.0, 65.8, 64.0 (O*C*H *asym*), 59.2 (N*C*H_2 *sym*), 66.6, 65.9, 65.9 (N*C*H_2 *asym*), 20.4 (*C*H_3 *sym*), 22.8, 20.7, 20.5 (*C*H_3 *asym*), 156.4, 128.6, 120.5, 119.6 (Ph*C*). IR (cm^{-1}): 1465 m, 1380 m, 1155 s, 1112 s, 1095 m, 885 s, 794s, 440 w. EI-MS: *m*/*z* (relative abundance, %) 309.4 (9) [M^+], 216.1 (100) [M^+-C_6H_5O].

4.2.5. $C_6H_5OSi[(OCH_2CH_2)_2\ (CH_2CH_2CH_2)]N$ (**10b**)

A mixture of 4.96 g (0.025 mol) γ-chloropropyltrimethoxysilane, 2.63 g (0.025 mol) diethanolamine, and 2.35 g (0.025 mol) phenol in xylene (25 mL) was heated to 100 °C. After adding KOH, the formed methanol was distilled off by means of a Marcusson device. After removing the device, 4.9 mL (0.035 mol) triethylamine was added and the reaction mixture refluxed for 20 h. The precipitated triethylamine hydrochloride was filtered off, the filtrate concentrated to dryness, and the residue recrystallised from *n*-hexane. Yield: 1.66 g (25%), m.p. 68–71 °C. Anal. Calc. for $C_{13}H_{19}NO_3Si$: C, 58.84; H, 7.22; N, 5.28; Si, 10.58. Found: C, 59.12; H, 7.48; N, 5,01; Si, 11.17%. $^{13}C\{^1H\}$ NMR ($CDCl_3$): δ 58.6 (3C O*C*H_2), 52.3 (2C N*C*H_2), 51.9 (N*C*H_2), 20.3 (C*C*H_2C), 8.4 (Si*C*H_2), 156.9, 128.7, 120.1, 119.4 (Ph*C*). IR (cm^{-1}): 1600 s, 1498 s, 1269 s, 1169 s, 1119 s, 1105 s, 920 k, 880 s, 790 s, 772 s, 760 s, 690 s, 590 w. EI-MS: *m*/*z* (relative abundance, %) 265.1 (10) [M^+], 172.2 (100) [M^+-C_6H_5O].

Acknowledgements

We thank Prof. A.K. Powell for the use of X-ray diffractometers, and Prof. J. Fekete for his valuable contribution in the chromatographic work.

Appendix A. Supplementary material

CCDC 678878, 678879, 678880 contain the supplementary crystallographic data for this paper. These data can be obtained free of charge from The Cambridge Crystallographic Data Centre via www.ccdc.cam.ac.uk/data_request/cif. Supplementary material associated with this article can be found, in the online version, at doi:10.1016/j.jorganchem.2008.09.055.

References

[1] (a) P. Hencsei, L. Párkányi, Rev. Silicon, Germanium, Tin and Lead Comp. 8 (1985) 191;
(b) R.J.P. Corriu, J. Organomet. Chem. 400 (1990) 81;
(c) M.W. Schmidt, T.L. Windus, M.S. Gordon, J. Am. Chem. Soc. 117 (1995) 7480;
(d) J.M. Anglada, C. Bo, J.M. Bofill, R. Crehuet, J.M. Poblet, Organometallics 18 (1999) 5584;
(e) A.B. Trofimov, V.G. Zakrzewski, O. Dolgounitcheva, J.V. Ortiz, V.F. Sidorkin, E.F. Belogolova, M. Belogolov, V.A. Pestunovich, J. Am. Chem. Soc. 127 (2005) 986;
(f) M.V. Zabalov, S.S. Karlov, G.S. Zaitseva, D.A. Lemenovskii, Russ. Chem. Bull. 55 (2006) 464.
[2] (a) Q. Shen, R.L. Hilderbrandt, J. Mol. Struct. 64 (1980) 257;
(b) G. Forgács, M. Kolonits, I. Hargittai, Struct. Chem. 1 (1990) 245.
[3] (a) A. Chandrasekaran, R.O. Day, R.R. Holmes, J. Am. Chem. Soc. 122 (2000) 1066;
(b) M.G. Voronkov, A.N. Egorochkin, O.V. Kuznetsova, J. Organomet. Chem. 691 (2006) 159;
(c) A.N. Egorochkin, M.G. Voronkov, O.V. Kuznetsova, O.V. Novikova, J. Organomet. Chem. 693 (2008) 181.
[4] (a) M.G. Voronkov, V.M. Dyakov, S.V. Kirchipenko, J. Organomet. Chem. 233 (1982) 1. and references cited therein;
(b) S.N. Tandura, M.G. Voronkov, N.V. Alekseev, Top. Curr. Chem. 131 (1986) 99.
[5] (a) M.G. Voronkov, Top. Curr. Chem. 84 (1979) 77;
(b) L. Bihátsi, P. Hencsei, L. Kótai, G. Ripka, Növényvédelem 28 (1992) 180;
(c) L. Zhonghua, S. Xiuyan, S. Huaping, C. Jing, Heterocyclic Commun. 11 (2005) 475;
(d) A. Zablotskaya, I. Segal, S. Belyakov, E. Lukevics, Appl. Organomet. Chem. 20 (2006) 149.
[6] (a) N. Kuanchertchoo, S. Kulprathipanja, P. Aungkavattana, D. Atong, K. Hemra, T. Rirksomboon, S. Wongkasemjit, Appl. Organomet. Chem. 20 (2006) 775;
(b) N. Thanabodeekij, S. Sadthayanon, E. Gulari, S. Wongkasemjit, Mater. Chem. Phys. 98 (2006) 131;
(c) N. Kritchayanon, N. Thanabodeekij, S. Jitkarnka, A.M. Jamieson, S. Wongkasemjit, Appl. Organomet. Chem. 20 (2006) 155.
[7] C.L. Frye, G.E. Vogel, J.A. Hall, J. Am. Chem. Soc. 83 (1961) 996.
[8] M.G. Voronkov, G.I. Zelchan, Khim. Geteroc. Soed. (1966) 511.
[9] E. Lukevics, L.I. Libert, M.G. Voronkov, Zh. Obshch. Khim. 39 (1969) 1784.
[10] L. Bihátsi, P. Hencsei, I. Kovács, L. Kótai, HU 210806, December 01, 1989 [C.A. 1991, 115:280295].
[11] L. Párkányi, P. Hencsei, L. Bihátsi, I. Kovács, A. Szöllősy, Polyhedron 4 (1985) 243.
[12] L. Párkányi, V. Fülüp, P. Hencsei, I. Kovács, J. Organomet. Chem. 418 (1991) 173.
[13] (a) J.W. Turley, F.P. Boer, J. Am. Chem. Soc. 90 (1968) 4026;
(b) L. Párkányi, K. Simon, J. Nagy, Acta Crystallogr. B 30 (1974) 2328;
(c) L. Párkányi, J. Nagy, K. Simon, J. Organomet. Chem. 101 (1975) 11.
[14] (a) A. Greenberg, G. Wu, Struct. Chem. 1 (1991) 79;
(b) P. Hencsei, Struct. Chem. 2 (1991) 21.
[15] (a) R.K. Harris, B.E. Mann (Eds.), NMR and the Periodic Table, Academic Press, London, New York, San Francisco, 1978;
(b) V.A. Pestunovich, S.N. Tandura, M.G. Voronkov, G. Engelhardt, E. Lippmaa, T. Pehk, V.F. Sidorkin, G.I. Zelchan, V.P. Baryshok, Dokl. Akad. Nauk SSSR 240 (1978) 914.
[16] (a) M.G. Voronkov, Pure Appl. Chem. 13 (1966) 35;
(b) J.M. Bellama, J.D. Nies, N. Ben-Zvi, Magn. Reson. Chem. 240 (1986) 748.

[17] (a) Programs WinDaisy and WinNmr, Bruker Daltonik, Bremen, Germany, 1999;
(b) G. Hägele, M. Engelhardt, W. Boenigk, Simulation und automatisierte Analyse von Kernresonanzspektren, VCH, Weinheim, Germany, 1987.

[18] (a) G.M. Sheldrick, SHELXS-97, Program for Crystal Structure Solution, University of Göttingen, Germany, 1997;
(b) G.M. Sheldrick, SHELXL-97, Program for Crystal Structure Refinement, University of Göttingen, Germany, 1997.